Additive Manufacturing 25 (2019) 166–175

Contents lists available at ScienceDirect

Additive Manufacturing

journal homepage: www.elsevier.com/locate/addma

Geometrical effects on residual stress in selective laser melting

L.A. Parry, I.A. Ashcroft*, R.D. Wildman

Centre for Additive Manufacturing, Faculty of Engineering, University of Nottingham, Nottingham NG7 2RD, UK

ARTICLE INFO

Keywords:
Selective laser melting
Residual stress
simulation
Laser scan strategy

ABSTRACT

Selective laser melting is an increasingly attractive technology for the manufacture of complex and low volume/high value metal parts. However, the inevitable residual stresses that are generated can lead to defects or build failure. Due to the complexity of this process, efficient and accurate prediction of residual stress in large components remains challenging. For the development of predictive models of residual stress, knowledge on their generation is needed. This study investigates the geometrical effect of scan strategy on residual stress development. It was found that the arrangement of scan vectors due to geometry, heavily influenced the thermal history within a part, which in turn significantly affected the transverse residual stresses generated. However, irrespective of the choice of scanned geometry and the thermal history, the higher magnitude longitudinal stresses had consistent behaviour based on the scan vector length. It was shown that the laser scan strategy becomes less important for scan vector length beyond 3 mm. Together, these findings, provide a route towards optimising scan strategies at the *meso*-scale, and additionally, developing a model abstraction for predicting residual stress based on scan vectors alone.

1. Introduction

Residual stress is inherent to thermal manufacturing processes, and parts manufactured using selective laser melting (SLM) are especially susceptible to build defects and potentially build failure associated with residual stress during processing. This includes the creation of surface defects, porosity, part distortion and under extreme situations delamination of the part from its support structures. Temperature gradients created in SLM drive the creation of high residual stress [1].The ability to predict the residual stress, and associated distortion prior to manufacture when designing industrial sized parts is vital for this technology to become successful [2,3].

The study of the thermo-mechanical behaviour in SLM is challenging, owing to the time and length scales involved in the process. Performing experiments to investigate the thermo-physical phenomena in the laser process zone, and specifically the build-up of transient residual stresses in-process remains limited due to the resolution, cost, and accessibility offered by currently available measurement techniques [4,5].

It has been shown that the magnitude of the longitudinal residual stresses generated parallel to the scan vectors in SLM is highly dependent on the scan vector length [1,6–8]. Also it found the transient thermal effects during processing affected the distribution and magnitude of the transverse stress component generated perpendicular to the scan vector [8]. However, no reported literature to date investigated the geometrical arrangement of scan vectors on residual stress. This paper defines ‘scan vector geometry’ as the overall shape rastered by a specific arrangement of scan vectors. The same shape may infact be hatched differently which results in a different arrangement of scan vectors.

In the literature, the investigation of scan strategies was undertaken on square island geometries, which always featured a constant scan vector length parallel to the island edge [9–11,8]. This is a simplified test case and is only encountered in scanning regions with a large cross-sectional areas. It is proposed that under certain situations, the choice of scan vector geometry could have a localised heating effect within hatch regions, such as corners of geometry as illustrated in Fig. 1. This could potentially result in excess heat build-up within localised regions, which could in turn affect the stability of the process. Additionally, it is suspected that the thermal history with varying scan vector geometry profiles could affect the generation of residual stress.

The accurate prediction of residual stresses and distortion typically involves modelling the path of a moving laser across the powder bed using a non-linear thermo-mechanical model. This is computationally expensive and tends to be limited to small regions. Multi-scale approaches present an opportunity to reduce the complexity of the problem to manageable computational demand [2,11]. Currently proposed multi-scale approaches use an ‘inherent strain’ technique, or

* Corresponding author.
E-mail address: ian.ashcroft@nottingham.ac.uk (I.A. Ashcroft).

https://doi.org/10.1016/j.addma.2018.09.026
Received 15 June 2018; Received in revised form 22 September 2018; Accepted 23 September 2018
Available online 25 September 2018

Nomenclature

h_d	hatch distance [mm]
L_T	layer thickness [mm]
P	nominal laser power [W]
r_d	laser spot radius [mm]
T	temperature [°C]
v	effective laser scan speed [mm/s]
α	thermal diffusivity [m^2/s]
α_{CTE}	linear coefficient of thermal expansion
η	laser efficiency
ϕ	state variable
σ	stress [MPa]
σ_y	yield stress [MPa]
θ_h	hatch angle [°]

substitution of a resolved stress field from a *meso*-scale region using a thermo-mechanical model, and incorporation of this at the *macro*-scale. This provides a prediction of the final resolved residual stress and distortion in a component. These approaches still require calculation of the stress field for these *meso*-scale regions, appropriate for the material, the machine, and the laser parameters. An improvement on these models would be the capability to predict the residual stress distribution based on the scan vectors alone. This would provide an opportunity to create a simpler multi-scale representation, suitable for predicting residual stress and distortion in components.

In this paper, a thermo-mechanical finite element model is used to investigate the effects of scan vector geometry on the thermal history created and their impact on the residual stress generated in a single layer. The knowledge gained reveals the methods by which residual stress is generated. Potentially, this could be used to develop a simplified method of predicting residual stress based on the scan geometry alone, which could be incorporated into a multi-scale modelling strategy. It also provides routes to further optimise the scan vector geometry used in order to minimise overheating and residual stress in *meso*-scale regions.

2. Methodology

A numerical simulation was used to investigate the effect of laser scan strategy on the SLM of Ti-6Al-4V. The following parameters were used for the simulation: layer thickness $L_T = 40\,\mu m$, hatch distance $h_d = 0.09\,mm$, laser power $P = 80\,W$ and laser speed $v = 500\,mm/s$. These correspond to parameters used on a Realizer SLM 50 system.

2.1. Thermo-mechanical finite element model definition

This study used a previously created coupled finite element thermo-mechanical model developed in MSC Marc, which incorporated additional user-defined subroutines for octree adaptive meshing [8,12]. The model, shown in Fig. 2, used a moving volumetric Gaussian heat source applied to the surface of a single powder bed layer. The powder bed included convective, and radiation heat losses at the surface. A fixed temperature of 200 °C for the preheated bed was applied to the bottom surface of the substrate. The thermal analysis was coupled with a mechanical analysis that used an elasto-plastic constitutive model, with kinematic work hardening. A fixed displacement boundary condition was applied to the bottom surface of the solid substrate.

The powder bed continuum consists of three material phases (powder, solid, liquid) with temperature dependent thermo-physical properties, and absorptivity conditions for Ti-6Al-4V [8]. The state and transformation between phases was tracked using a state variable ϕ with the definition

$$\phi = \begin{cases} -1 & \text{Liquid state} \\ 0 & \text{Powder state} \\ 1 & \text{Solid state} \end{cases}, \tag{1}$$

Material properties were linearly interpolated between those defined at the powder and solid phase ($0 \le \phi \le 1$) and it was assumed that there was negligible mechanical interaction of the powder phase [10]. Therefore the mechanical material properties were scaled for the powder phase using the factors in Table 1.

Adaptive octree mesh refinement was used to significantly increase the simulation throughput whilst preserving discretisation accuracy in the regions of thermal gradients which generate residual stresses. Elements were a minimum element length of 0.02 mm within a radial distance from the laser spot, to capture the high thermal gradients within the melt-pool. An additional refinement was made on solid elements ($\phi = 1$), determined by the maximum absolute component of the temperature gradient on such that

$$\max \left| \frac{\partial T}{\partial x_i} \right| > f_{\text{grad}}\,, \tag{2}$$

with the refinement parameter $f_{grad} = 500$. When the criterion was not met, an un-refinement procedure coarsened previously refined elements to an intermediate size (0.08 mm), to improve the performance of the simulation.

In order to conduct a large number of simulations, the analyses were performed using the University of Nottingham's Minerva high performance computing facilities.

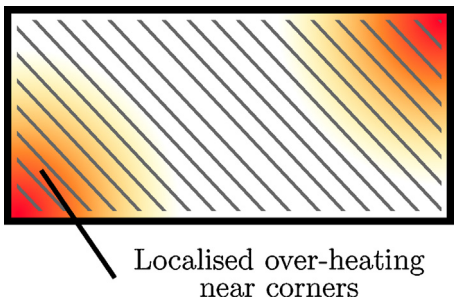

Fig. 1. Illustration showing the localised build-up of heat created when scanning towards the corners of geometries.

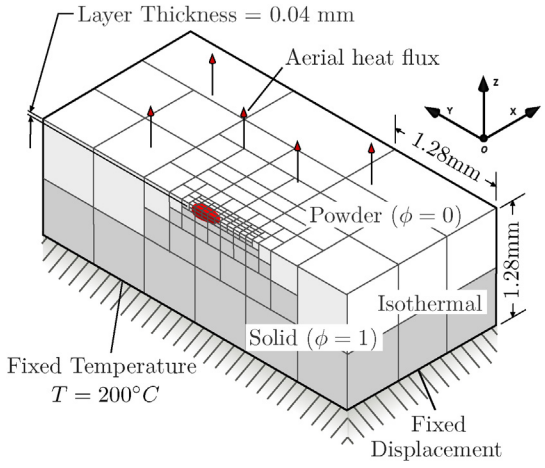

Fig. 2. Illustration of the adaptive-mesh and boundary conditions used for the thermo-mechanical analysis.

Table 1
Scale factors used for relating the mechanical properties of powder phase with the solid phase.

Property	Scale factor
Young's Modulus E	0.1
Thermal expansion coefficient α_{CTE}	0.1
Yield stress σ_y	0.1

2.2. Geometry chosen in this study

In order to understand the role of geometry dependency in relation to the scan strategy, a series of geometrical primitives (triangles and squares) of different aspect ratios was considered. The use of triangles creates scan vectors with lengths that vary linearly across the geometry, at a rate dependent on the aspect ratio chosen. This will enable the characterisation of the influence of the thermal history of a scanned region on the build-up of residual stresses caused by the previously accumulated heat.

Both the triangles and squares had a maximum length $l = 5$ mm, and their size varied, using ten different aspect ratios by changing the height h, as illustrated in Fig. 3. The triangles were hatched in two directions, to fully explore the effect of scan strategy on different aspect ratio geometry.

2.2.1. Optimising the scan strategy

Typically scan strategies are sorted arbitrarily and are oriented layer-wise in order to improve the homogeneity of the microstructure with parts manufactured. In the literature, there has been no study that has attempted to optimise orientation and scan-order. A hypothesis was formed that reducing the overall mean and variance of the scan vector length could reduce the overall magnitude of residual stresses within a region. Additionally, reducing the variance could reduce the risk for creating localised zones with an excess build-up of heat. In order to determine the validity of the hypotheses, a simple geometrical test was performed by varying the hatch angle when hatching different aspect ratio triangles, where $\theta_h = 0$ corresponds to horizontal hatching. This resulted in the distribution of scan vector lengths with varying angles shown in Fig. 4.

Performing the geometrical test for the triangles, it was observed that irrespective of aspect ratio, the local minima for the mean and variance was found when the hatch angle was perpendicular to the triangle's hypotenuse. Based on this knowledge, another set of test cases were developed with the hatch angle perpendicular to the hypotenuse, as shown in Fig. 5(d).

For this investigation, 40 primitive geometries were considered to understand the geometrical effect of scan strategy. The collections of hatched primitives are shown in Fig. 5 using a larger hatch distance for illustration.

In order to examine the transverse and longitudinal residual stress distributions generated across the geometries, the σ_{xx} and σ_{yy} stress fields were extracted from the results when the scanned region cooled to a uniform temperature of 200 °C. The stress fields were exported to Matlab using a *Python* script within the active layer and the layer below the scanned region ($-L_T < z < L_T$).

3. Results

The stress distribution plots for all the analyses are shown in Fig. 6. It is clear from the triangle geometries shown in Fig. 6(a–c), that the orientation of the scan vector used for hatching geometrical primitives has a significant effect on the magnitude and distribution of residual stresses. The aspect ratio of the scanned shape determines the overall magnitude of the residual stresses generated, since this primarily determines the scan vector length.

3.1. Residual stresses in triangular geometries

As seen in the surface contour plots of von Mises stress in Fig. 6, it appears that orientating the hatch angle to follow the hypotenuse of the triangle tends to reduce the magnitude of the residual stresses generated throughout the scanned geometry. The probability density function (PDF) of the von Mises stresses for each triangle test case with each hatch orientation is shown in Fig. 7. This plots shows that the peak of the stress using a perpendicular hatch remains narrow and stationary at ~450 MPa irrespective of the aspect ratio, except for the high aspect ratio cases (1.5 × 5.0, 2.0 × 5.0) mm. The narrow distribution observed for the perpendicular hatching, corresponds to low variance in the scan vector length.

The residual stress distribution using the horizontal and vertical hatching are more heavily influenced by the aspect ratio of the geometry. In the low aspect ratio, triangular geometries (Fig. 7(f)–(h)), the distribution of the stresses for both the vertical and horizontal hatching become bi-modal. Of the two peaks, the higher magnitude peak is associated with regions of long scan vector lengths whilst the smaller magnitude peak is associated with the shorter scan vectors towards the end of scanning the geometry. Generally, horizontal hatching results in higher magnitude of residual stress for the given area, especially for high aspect triangles, as shown in Fig. 7(a)–(c). This is expected to be caused by these scanned geometry cases always having a full scan vector length (5 mm) along the bottom edge. When using the vertical hatching, the maximum length of the scan vectors are based on the shortest length of the triangle. In the higher aspect ratios, higher magnitudes of residual stresses are generated towards the corner of the triangle (regions with shorter scan vectors). It would be expected that these regions would also suffer from the effect of localised over-heating. This can be observed when comparing the temperature distribution towards the shortest scan vectors at the acute angle of the triangle for the (2.0 × 5.0) mm triangles between horizontal and vertical hatching in Fig. 8(a) and (b).

The distribution of the stresses within the triangles scanned using the horizontal and vertical hatching tend to be similar in shape, as demonstrated in all the cases in Fig. 7(a) and in Fig. 7(b). The peaks of the longitudinal and transverse stresses tended to be located through a line X-X extending through the triangle's centroid, as shown in Fig. 9(a).

The transverse and longitudinal residual stresses generated in the geometries of different aspect ratios are plotted against the distance along line X-X normalised with the effective scan vector length in

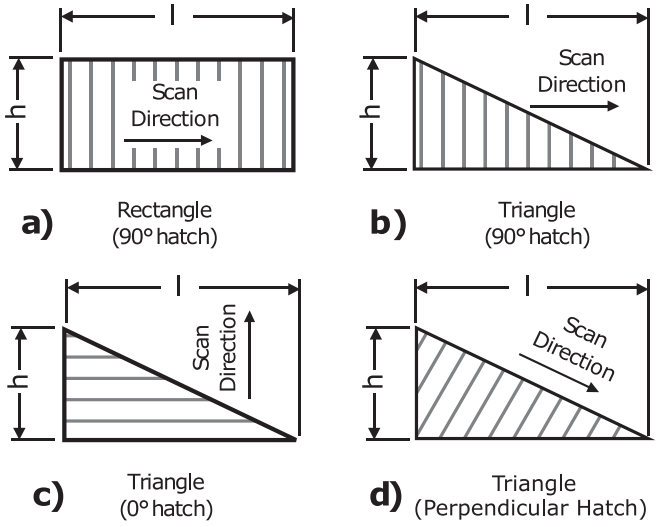

Fig. 3. Illustration showing the geometrical test cases with varying length h: (a) rectangle hatched vertically, and triangles hatched at (b) vertically, (c) horizontally, and (d) perpendicular to hypotenuse.

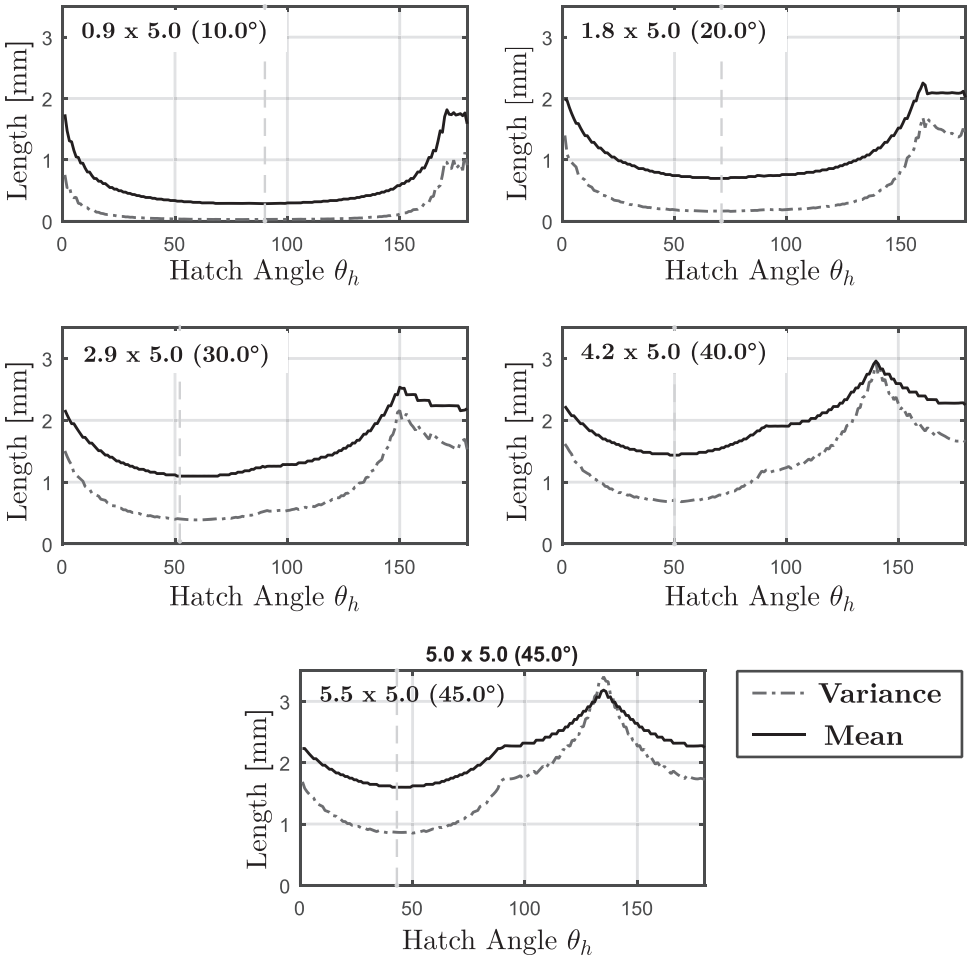

Fig. 4. Graphs of the mean and variance of the scan vector lengths against the hatch angle θ_h for different aspect ratio triangles.

Fig. 10 for the vertical hatching, and Fig. 11 for the horizontal hatching. It can be seen in both Fig. 10(b) and Fig. 11(b) that the longitudinal stresses increased linearly with the scan vector length, and begin to plateau when the scan vector length becomes greater than 3 mm.

The transverse residual stresses generated perpendicular to the scan vectors vary considerably, irrespective of the aspect ratio and hatch angle, as shown in Fig. 10(a) and Fig. 11(b). Reducing the effective scan vector length increases the magnitude of the transverse stresses which plateau towards a limit depending on the aspect ratio of the triangle chosen. This shows the strong influence of previous thermal history on the generation of the transverse stresses within a structure which is specific to the geometry scanned.

3.2. Residual stresses in rectangular geometries

The transverse and longitudinal residual stresses generated in the

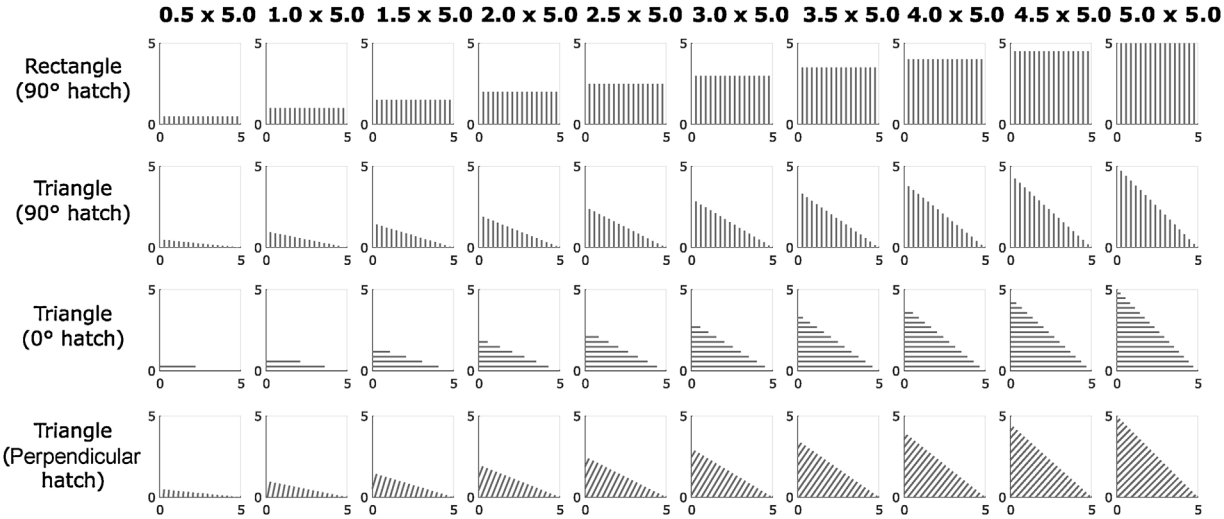

Fig. 5. The hatched geometrical primitives generated, which are scanned from left to right. For illustration, the hatch spacing has been increased.

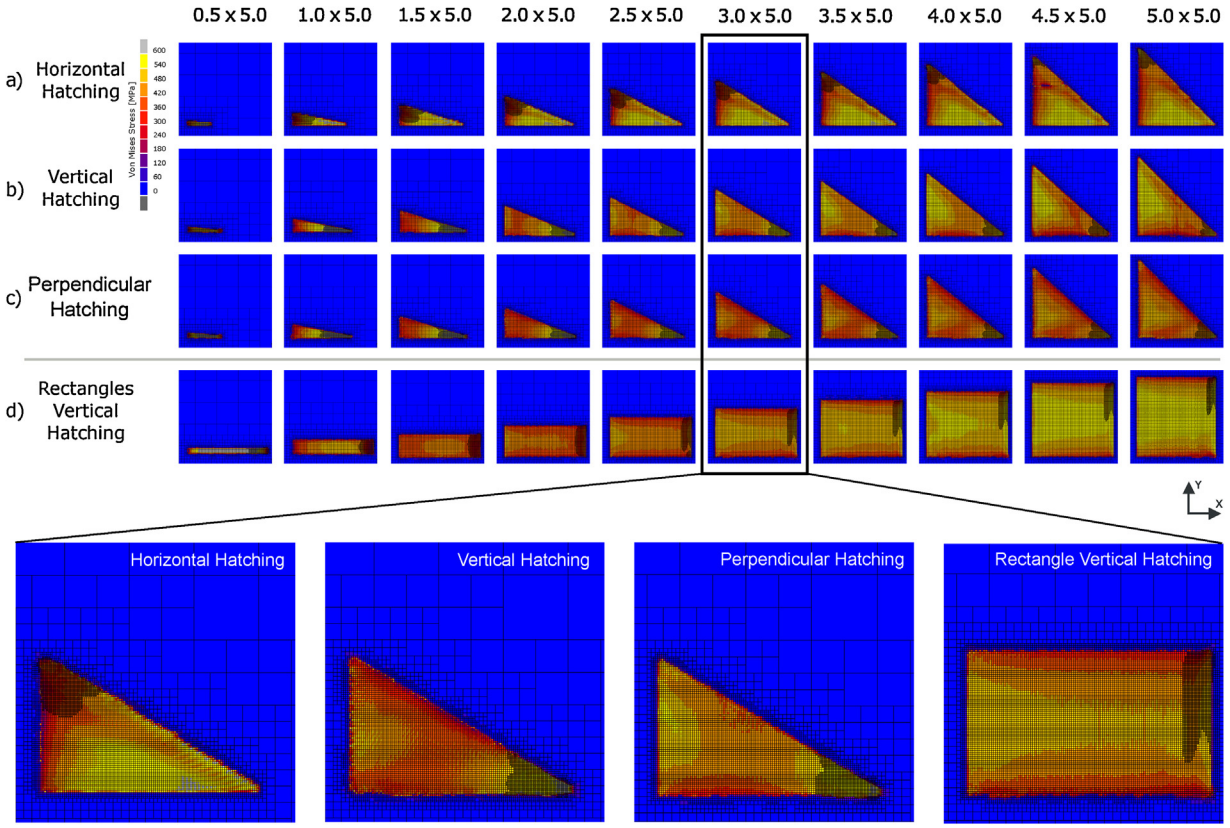

Fig. 6. Profile views showing the von Mises stress distribution of scanned triangle primitives with (a) horizontal hatching, (b) vertical hatching, (c) perpendicular hatching, and (d) rectangles hatched vertically.

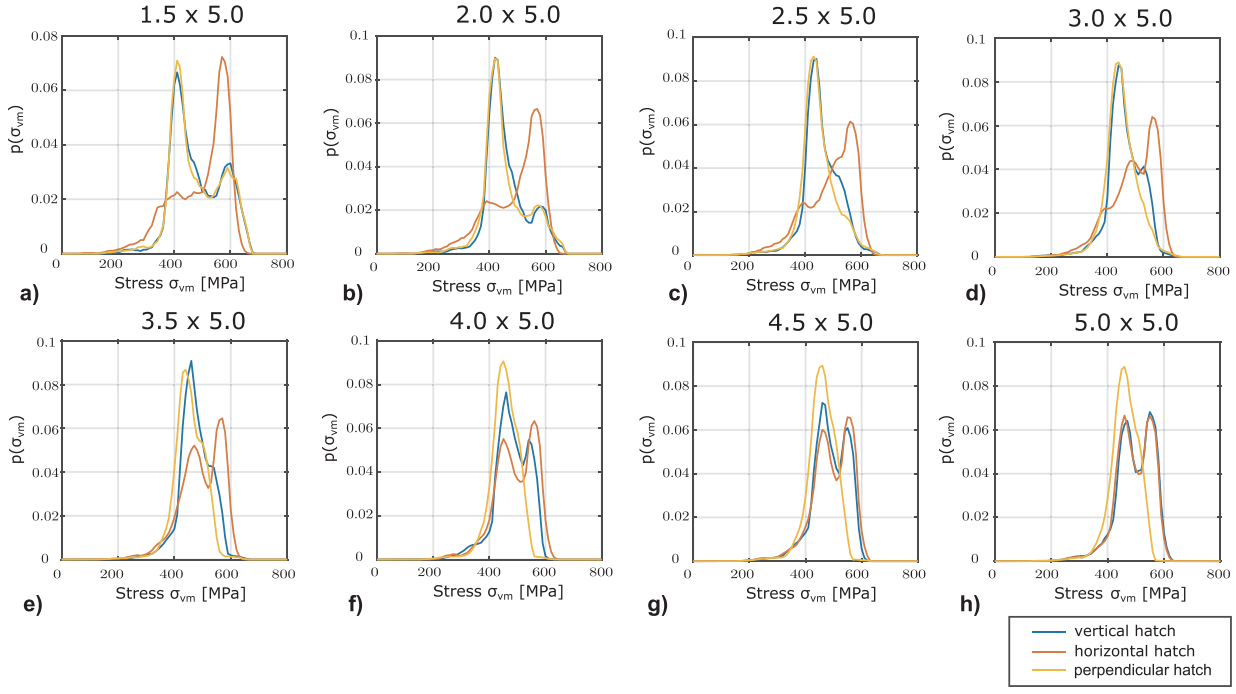

Fig. 7. Comparison of the von Mises PDFs $p(\sigma_{vm})$ for the different aspect ratio triangles using the horizontal, vertical and perpendicular hatching.

rectangular geometries were sampled across the centre, and their distributions are shown in Fig. 12. The transverse stresses (Fig. 12(a)) generally have a slightly asymmetric, flat profile along the width of the rectangular geometry, which decreases rapidly at the far edges. This rapid decrease in the transverse stress can be attributed to the fact that transverse stresses are not generated towards the end of scanning the region. The curvature of the transverse stress distribution (Fig. 12(a)) along the central profile of the rectangular geometries is associated with the resultant deformation of the layer at this temperature (200 °C). Using the shortest scan vectors, ranged between 1.5 and 2.5 mm,

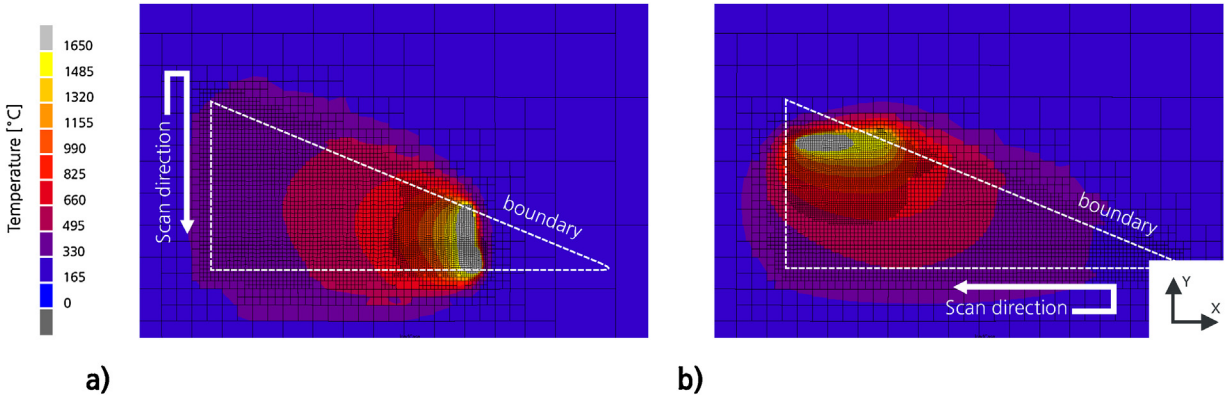

Fig. 8. Profile of the surface showing the temperature distribution towards the end of scanning for a (2 × 5) mm triangle using a (a) vertical hatching and (b) horizontal hatching.

significantly increased the magnitude of the transverse stresses generated. For the longer scan vectors, the magnitude of transverse stresses varied by ~30 MPa. This shows similarities with the observations of the residual stresses generated in high aspect ratio triangles.

The longitudinal stresses shown in Fig. 12(b) reduced from the highest point at the start of scanning before tending towards a constant stress value dependent on the scan vector length. This largest decrease at the beginning of scanning was observed using the shortest scan vector lengths between 1.5 and 2.5 mm. This could be attributed to an overheating effect due to the lack of material available at the beginning of a scan for the dissipation of heat.

The difference in magnitude between the longitudinal and transverse stresses sampled for all aspect ratio triangles hatched vertically are shown in Fig. 13. For all aspect ratio triangles, an equiaxial stress was observed at a critical scan vector length between 1.7 and 2.3 mm. Below this critical scan vector length, the greater contributions from the transverse stress dominate, and above this length the longitudinal stresses steadily increase the difference between stress components.

3.3. Thermal history of the scanned geometries

In order to examine the thermal history on the effect of the build-up of the transverse residual stresses, the mean temperature of consolidated elements ($\phi = 1$) in the scanned layer was plotted against the scan time in Fig. 14. The temperature profile plot showed that irrespective of geometry, increasing the area scanned or the effective scan length tended to reduce the mean temperature across the entire duration of scanning. The rectangular cases with scan vector lengths < 2.5 mm experienced the highest sustained average temperatures.

Shorter scan vectors such as those in the rectangular case in Fig. 14(c) may initially have the highest average temperatures but experienced a higher rate of temperature loss across the normalised scanning duration. For the rectangles which have constant scan vector lengths, the average temperature decreased linearly with time.

When comparing the mean temperature of the rectangles (Fig. 14(c)) with the transverse residual stress generated (Fig. 12(a)) for the shortest scan vector lengths [1.5–2.5] mm, the transverse stress continued to increase until the mean temperature was approximately 750 °C. The transverse residual stress for greater scan vector lengths settles towards ~300 MPa, and it can be observed that the mean temperature for these sizes remain below ~750 °C.

4. Discussion

Numerous simulations of geometric shapes were analysed by

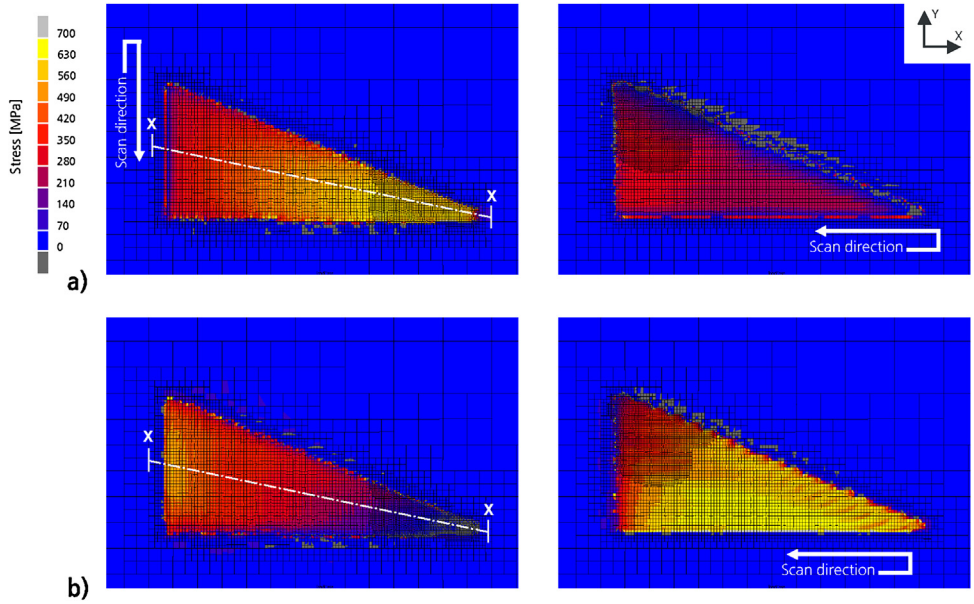

Fig. 9. Profile of the surface showing (a) the transverse and (b) longitudinal stresses using vertical hatching (left), and horizontal hatching (right) for the (2 × 5) mm triangle geometry.

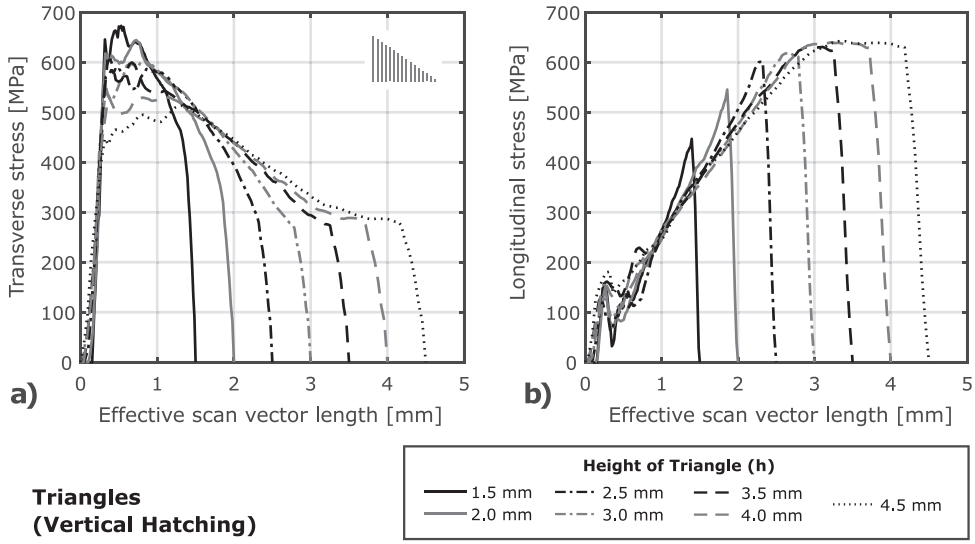

Fig. 10. Graph showing (a) the transverse and (b) the longitudinal stresses plotted against the effective scan vector length when scanning different aspect ratio triangles with vertical hatching.

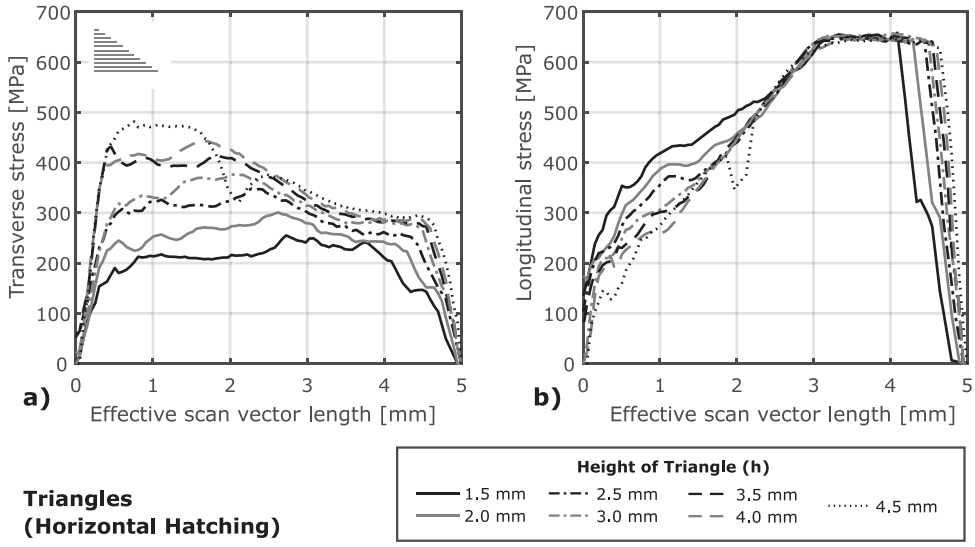

Fig. 11. Graph showing (a) the transverse and (b) the longitudinal stresses plotted against the effective scan vector length when scanning different aspect ratio triangles with horizontal hatching.

scanning different aspect-ratio triangle and rectangular primitives in order to determine the effect of geometry on the generation of residual stress, as shown in Fig. 6. It was confirmed that as expected scan vector length plays a significant role in the magnitude of stresses generated, as shown previously in the literature [1,7,8].

4.1. Residual stress in triangle geometries

For assessing any geometrical relationships with the residual stress generated, the profiles of the stress distributions taken through the triangle's centroid were analysed with respect to the effective scan vector length for different aspect ratio geometries. The transverse residual stresses generated perpendicular to the scan vectors varied considerably especially at short scan vector lengths irrespective of the aspect ratio, as shown in Fig. 10(a) and Fig. 11(a). There is a strong indication that the thermal history significantly affects the distribution transverse stress generated which does not correspond necessarily with the scan vector length, which was shown in previous work [8].

Previously, a hypothesis formed was that reducing the mean effective length of the scan vectors, could reduce the residual stresses generated. This was achieved by rotating the hatch angle to be perpendicular to the triangle's hypotenuse. It was found the overall magnitude of stress remained constant at approximately 430 MPa irrespective of the aspect ratio of triangle scanned. The results supported the hypothesis, however, a more systematic optimisation study is required to tune the scan orientation and order. This will enable developing an optimal approach towards reducing residual stress within a *meso*-scale region.

Irrespective of geometry, the longitudinal stresses, as shown in both Fig. 10(b), Fig. 11(b) increased linearly with scan vector length, then plateauing at 650 MPa with a scan vector length of approximately 3 mm. Shorter scan vectors between 1.5–2.5 mm are susceptible to overheating effects at the start of scanning. This is an important result because this provides predictable behaviour for the longitudinal stresses which linearly increases upwards to ~3 mm irrespective of the thermal history.

The residual stress anisotropy, which is the difference in magnitude between the longitudinal and transverse stresses for all aspect ratio triangles is shown in Fig. 13. This plot indicated that there is a critical scan vector length between 1.7–2.3 mm, which has the lowest residual

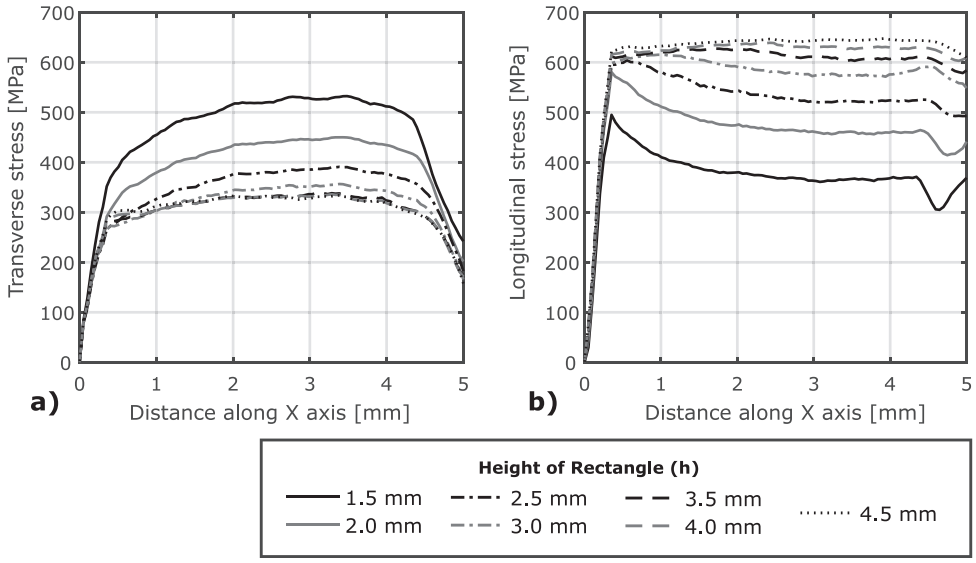

Fig. 12. Graph showing (a) the transverse and (b) the longitudinal stresses with distance across the central *X*-axis when scanning different aspect ratio rectangles with vertical hatching.

stress anisotropy. The importance of this is that the level of anisotropy for the residuals stresses generated within the layer plane could potentially be controlled by varying the directionality and the length of the scan vectors chosen within a region. However, it is expected that observations for the generation of residual stresses using scan vectors that are adjacent to each other will behave differently to more complex scan strategies.

4.2. Residual stress in rectangular geometries

The rectangular geometries investigated correspond to those using a 'stripe' scan strategy. The results shown in Fig. 12 indicate that the magnitude for both transverse and longitudinal stresses will remain constant along the length of the stripe, except for at the edges due to discontinuity of scanning. For shorter scan vector lengths, the thermal history had more of an effect on the stresses generated towards the start of scanning. Overall, the magnitudes of the longitudinal and to a lesser extent the transverse residual stresses in the stripes are determined by the scan vector length. Generally, both components of residual stress remain constant along the length of the stripe when scanning on a substrate. This result is significant because multi-scale modelling approaches [11] do not necessarily require explicit modelling of each meso-scale regions (islands or stripes).

4.3. Effect of thermal history on residual stress generated

It was seen in Fig. 14, that the mean temperatures remained high ($> 750\,^{\circ}C$) for short scan vectors [1.5–2.5] mm when scanning the rectangular geometries and this resulted in higher transverse residual stresses. This over-heating effect is not seen with lower aspect ratio geometries, because there is greater surface area for heat dissipation into the previously scanned region. It is proposed that changing the order of scanning by starting in the acute section of the triangle will affect the distribution of the transverse stress generated because there is previously less consolidated material for any heat to dissipate away into. This effect has not been reported in the literature, although typically short scan vectors are not often used for manufacturing parts using SLM.

4.4. Recommendations

Based on the findings, it is recommend scan strategies are designed to minimise the variance of the scan vector length, and where possible limit the use of short scan vectors < 2.5 mm, which was shown to create an over-heating effect in narrow regions. This can be mitigated by choosing an appropriate localised hatch orientation or the order of their scanning. Ideally, the order of scanning in narrow features should

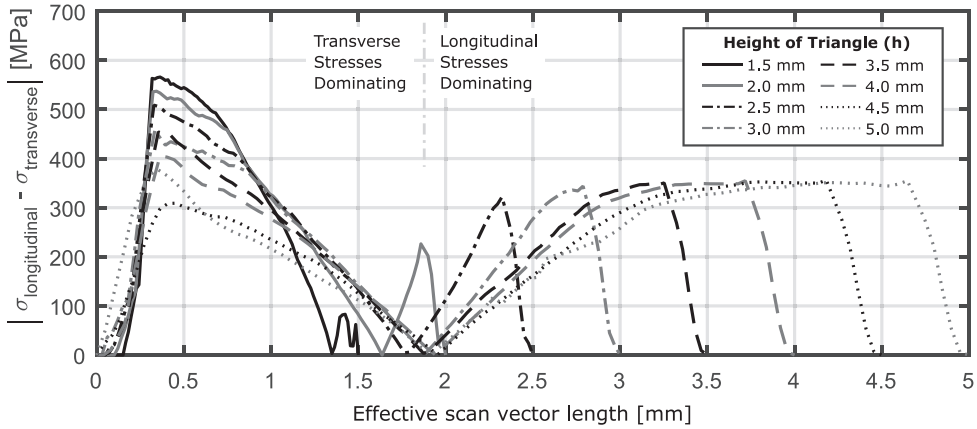

Fig. 13. Graph of the absolute difference between the transverse and longitudinal stress components against the effective scan vector length, when scanning different aspect ratio triangles.

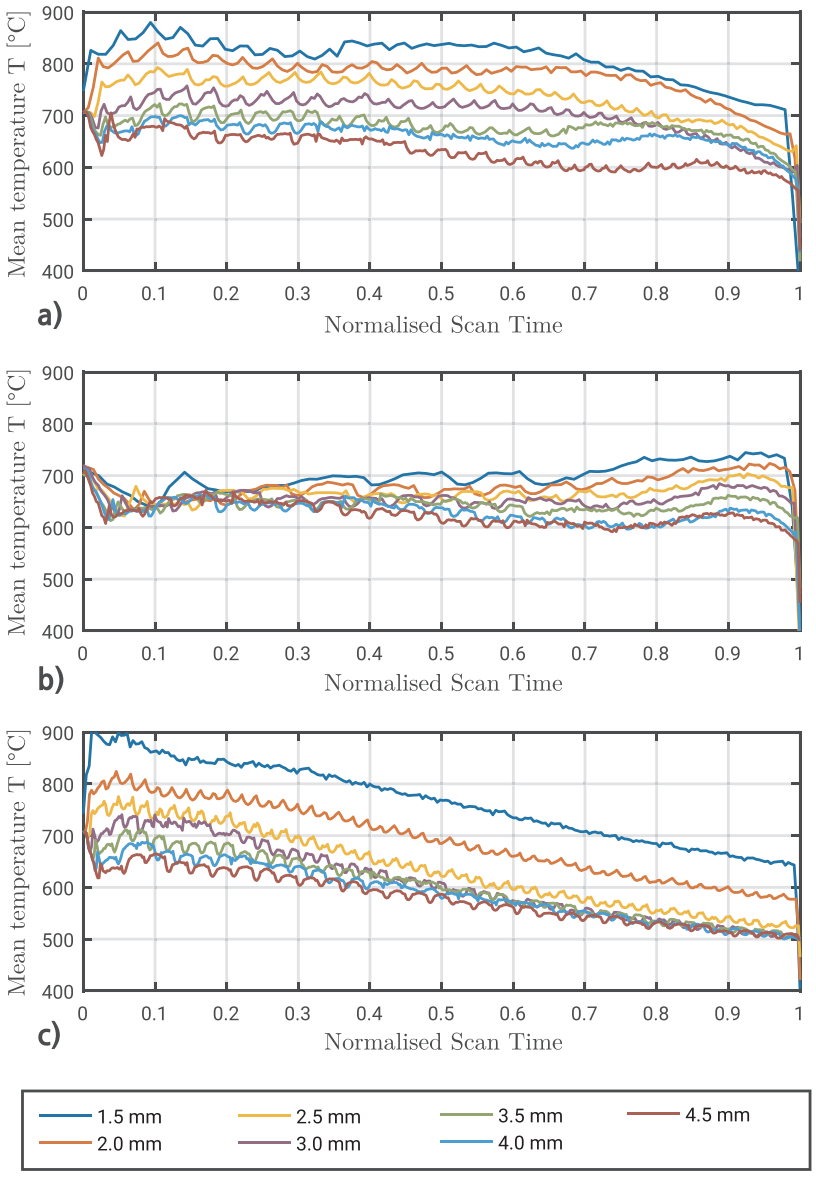

Fig. 14. Graph of the mean temperature of consolidated elements normalised to the scan time for triangles hatched (a) vertically, (b) horizontally, and (c) rectangles hatched vertically.

favour scanning larger-regions first (longer scan vectors) in order to use pre-consolidated regions for effectively dissipating excess heat. Other approaches could consider contour or border scanning in complex geometries e.g. lattice structures, or the use of watershed and bin packing algorithms to optimise the placement of hatches in complex regions. Overall, it is recommended to reduce the use of short adjacent scan vectors since these exasperate the effects of previous thermal history within the scanned region. It is expected that choosing scan vector lengths beyond 5 mm will have negligible impact on the magnitude of the longitudinal stresses generated. Therefore, using island sizes beyond 5 mm are unlikely to yield any reduction in the magnitude of residual stresses generated, except changing the overall directionality of the stress throughout the entire scanned layer.

Ultimately, this study shows that the prediction of longitudinal stresses generated along the scan vectors is consistent and is determinable, whilst the generation of transverse stresses is more complex. In order to provide a predictive model for the generation of residual stresses within a layer, further analysis is needed to understand the effect of thermal history created by geometry and the scan order on the generation of transverse stresses. This investigation would need to find a relationship between the accumulation of heat in a scanned area over time, and the rate of change in scan vector length. Having a predictive model for the *meso*-scale generation of residual stress generation would enhance *multi*-scale strategies for predicting distortion and residual stress in industrial parts. Further work is required to model this study across multiple layers and observe the effect of different hatch angles on the same region and develop an experimental procedure to validate the results for capturing the residual stress state of *meso-scale* scanned geometries.

5. Conclusions

A thermo-mechanical finite element model was used to study the effect of geometry on the build-up of residual stress in SLM. This provided a chance to explore the relation between the static and dynamic changes in scan vector length on the generation of residual stress. It was shown that the thermal history was dependent on the arrangement of scan vectors chosen, for the same geometry. As a result, the thermal history had a marked effect on the residual stresses generated. Specific conclusions that can be drawn from the results are:

- Longitudinal stresses linearly increased with scan vector length before plateauing after a critical scan vector length of 3 mm, irrespective of geometry chosen.
- Longitudinal stresses were largely independent of thermal history except at the start of scanning.
- Transverse stresses were highly geometrically dependent owing to the different thermal histories.
- Transverse stresses were found to be significantly higher for short scan vectors (< 2.5 mm).
- Both the longitudinal and transverse stresses stabilise towards a constant value using a fixed scan vector length in the rectangular geometries – i.e. 'stripe' scan strategy.
- Regions that are susceptible to localised overheating increase the magnitude of residual stresses generated.

Laser scan strategy becomes less important for scan vector length beyond 3 mm scan vector lengths in terms of the magnitude of residual stress generated. At the *macro*-scale, the distribution and orientation of scan vectors in relation to geometry becomes a more important consideration.

Acknowledgements

This work was supported by the Engineering and Physical Sciences Research Council [grant number EP/P027261/1]. We are also grateful for access to the University of Nottingham High Performance Computing Facility, which provided the capability to perform the thermo-mechanical simulation of this scale.

References

[1] P. Mercelis, J.-P. Kruth, Residual stresses in selective laser sintering and selective laser melting, Rapid Prototyp. J. 12 (October) (2006) 254–265.
[2] N. Keller, V. Ploshikhin, New method for fast predictions of residual stress and distortion of AM parts, Proceedings of the 24th Solid Freeform Fabrication Symposium, Austin, Texas, 2014, pp. 1229–1237.
[3] F. Neugebauer, N. Keller, H. Xu, C. Kober, V. Ploshikhin, Simulation of selective laser melting using process specific layer based meshing, Proceedings of the Fraunhofer Direct Digital Manufacturing Conference, Bremen Center for Computational Materials Science, Bremen, 2014.
[4] B. Vrancken, Study of Residual Stresses in Selective Laser Melting. PhD Thesis, KU Leuven, 2016.
[5] A.S. Wu, D.W. Brown, M. Kumar, G.F. Gallegos, W.E. King, An experimental investigation into additive manufacturing-induced residual stresses in 316L stainless steel, Metallurg. Mater. Trans. A: Phys. Metal. Mater. Sci. 45 (13) (2014) 6260–6270.
[6] H. Pohl, A. Simchi, M. Issa, H. Dias, Thermal stresses in direct metal laser sintering, Proceedings of the 12th Solid Freeform Fabrication Symposium, Austin, Texas, 2001, pp. 366–372.
[7] J.-P. Kruth, J. Deckers, E. Yasa, R. Wauthle, Assessing and comparing influencing factors of residual stresses in selective laser melting using a novel analysis method, Proc. Inst. Mech. Eng. Part B: J. Eng. Manuf. 226 (June) (2012) 980–991.
[8] L. Parry, I. Ashcroft, R. Wildman, Understanding the effect of laser scan strategy on residual stress in selective laser melting through thermo-mechanical simulation, Addit. Manuf. 12 (2016) 1–15.
[9] I.A. Roberts, Investigation of Residual Stresses in the Laser Melting of Metal Powders in Additive Layer. PhD Thesis, University of Wolverhampton, 2012.
[10] N.E. Hodge, R.M. Ferencz, J.M. Solberg, Implementation of a thermomechanical model for the simulation of selective laser melting, Comput. Mech. 54 (April) (2014) 33–51.
[11] C. Li, J.F. Liu, Y.B. Guo, Z.Y. Li, A temperature-thread multiscale modeling approach for efficient prediction of part distortion by selective laser melting, Proceedings of the 26th Annual International Solid Freeform Fabrication Symposium, Austin, Texas, USA, 2015.
[12] M.S. Corporation, MSC Marc, (2017).